Optic and electric methods and test procedures for the pulse spray parameters

A.D. Nazarov*, A.F. Serov, M.V. Bodrov, and V.A. Simakov
Siberian Branch of Russian Academy of Sciences
Institute of Thermophysics
Novosibirsk, Russia

Abstract

This report deals with the experience of application of optic observations and electric measurements for investigation of pulse spray parameters: size of liquid droplets, elongation of droplet area, and droplet grouping in the area with a distance from the source. The methods for measurement of liquid and gaseous phase uniformity in a cross-section of pulse spray are described.

Introduction

The spray is a type of non-uniform flows because it includes two components in different aggregate states. In contrast to homogeneous flows, which are characterized by one main parameter: mass velocity (average or local one), the heterogeneous flows are determined by some additional parameters: concentration and velocity of components, distribution of particle size and different ratios of these parameters.

At pulse spray generation the different-sized liquid particles moving with different velocities along the way of propagation are formed. The initial velocities of phases effect the length of the liquid droplet area and distribution of droplet mass concentration inside the droplet area.

The variety of studied parameters of the pulse spray has determined the complex approach of investigation, which combines the optic and electric methods of measurements of pulse spray characteristics.

Pulse source of spray

The controllable source [1] of a gas-droplet jet (Fig.1a) is made as the two-chamber unit: for water (1) and for air (2). On the flat part of the source there are 16 liquid sprayers in the form of 4×4 matrix (Fig.1b). On the same surface there are 25 gas nozzles with outlet diameter of 0.35 mm for generation of the co-current air flow. The liquid sprayer is a diffuser of four nozzles of the 125 um diameter, which are switched on by one electromagnetic valve (Fig.1c). The time of valve opening-closing cycle (and vice versa) is T_{tr} = 0.1 ms, what is less significantly than the time of valve opening at pulse spray formation during the experiment. Under operation conditions the time of valve opening is T_i = (0.002÷0.01) s and opening frequency is F_i = (1÷50) Hz. The liquid flow rate is determined by the pressure at the inlet of electromagnetic valve unit P_l = (0.05÷0.3) MPa, at this the liquid velocity in the flow is regulated within (0.5 ÷ 20) ms^{-1}. Programmable opening of valves allows formation of spray flows with different intensities by time and coordinate on the heat exchanger surface. The flow rate of gas component does not change in time for the specific conditions and it is determined by the pressure at the inlet to the air unit. The velocity of the co-current air flow can be determined (0÷20) ms^{-1} by a change in operation pressure P_g = (0÷0.6) MPa.

Methods and results of spray investigation

In the experimental series the heat exchanger and aerosol source were mounted vertically relative to the horizontal axis at the distance of 230 mm from each other. For this position in the cross-section of heat exchanger surface the source of the pulse gas-droplet flow forms the two-phase flow with the area of 300×300 mm.

A coordinate device was used for investigation of distribution of the air and liquid phases. A shift with accuracy of 20 um (shift error was 1×10^{-3}) was made along two coordinates by the step motors controlled by the software. The control equipment is made by the standard of KAMAK system. The link with a PC is performed via RS-232 interface. The control software is written in C++ language.

Uniformity of liquid phase distribution over the heat exchanging surface was controlled by a high-frequency electromagnetic meter [2]. The operation principle of this meter is based on absorption of energy, including the energy of electromagnetic field by the moving flow at field interaction with a water component of the aerosol flow. The source of electromagnetic oscillations is an emitter connected with a generator of high-frequency oscillations.

Density of energy in the electromagnetic wave is described by relationship [3]

* Corresponding author: nazarov@itp.nsc.ru

$$\omega = 1/8\pi(\boldsymbol{ED} + \boldsymbol{HB}), \quad (1)$$

where $\boldsymbol{E}$, V·m^{-1} is electric field strength; $\boldsymbol{D} = \varepsilon_0\varepsilon E$ is electric induction, $\varepsilon_0 = 8.85\times10^{-12}$ F·m^{-1} is electric constant, ε is medium permeability; $\boldsymbol{H}$, A·m^{-1} is magnetic field strength; $\boldsymbol{B} = \mu\mu_0 H$ is magnetic induction, $\mu_0 = 1.2\times10^{-12}$ H·m^{-1}, and μ is magnetic permeability of medium.

According to formula (1), a change in the density of electromagnetic energy is proportional to electric and magnetic properties of the ambient space near the emitter.

Magnetic properties of the flow stay constant at any relationships of water and air in this flow, and they do not change the value of electromagnetic energy. The density of high-frequency energy absorbed by the jet is determined only by electric properties of the flow. It is known [4] that dielectric permeability of water is 80 and permeability of air is 1. Thus, dielectric permeability of gas-droplet flow and absorbed energy of electromagnetic field depend mainly on water concentration.

The structural scheme of the device is shown in Fig.2a. A signal of generator (with frequency 433.92 MHz) is fed to the dipole emitter through the adapter circuit and amplifier. The device of automatic regulation keeps amplitude at the amplifier output constant. Information about electromagnetic energy absorbed by the medium near the emitter at interaction with the mixture is supplied to the summation unit via the detectors. An analogue signal is converted into the code by means of ADC controller, where this information is archived and can be fed either for indication or to a PC for the following processing and visual presentation of measurement results.

The length and measurement volume of emitter (Fig. 2b) were chosen by calculation of maximal radiation efficiency [5] and equaled 170 mm: the forth part of generator wavelength.

The emitter is a frame of three rods located parallel in one plane. The central rod (∅0.7 mm) is the emitter, and the external ones (∅3 mm) are connected with a screen. The free end of construction is fixed by an insulating fluoroplastic holder.

Before every next measurement (this is a disadvantage of this method) it is necessary to achieve total drying of the probe, otherwise, there will be reading uncertainty and error increase.

The measurement example of droplet phase (moisture) distribution in the pulse gas-droplet flow formed by the pulse spray source is shown in Figc. 3.

According to measurements of uniformity of phase distribution over a cross-section of the gas-droplet flow near the heat exchanger surface [2], deviations of liquid concentration from the average one do not exceed 5 % for the area equal to the heat exchanger surface despite scattering of individual flow rates of valves (10 %).

In this study the field of air flow velocities was scanned without liquid-droplet phase and in free space without heat exchanger. To perform measurements we have used the thermal anemometer “ATT-1004” registered in the public list of measurement instrumentations with the following characteristics: measurement range $V = (0.5 \div 20)$ m·s^{-1}; resolution of 0.1 m/s; and error of $\pm(0.05\cdot V + 0.2)$, where V is the measured value of the air flow velocity. The velocity field was measured for P_g = 0.05, 1.5 and 2 MPa. There was no significant change in the pattern of velocity distribution depending on a change in inlet pressure P_g = 0.05, 1.5 and 2 MPa; gas phase maldistribution depending on the average value was not worse than 5 %.

To observe droplet behavior at their motion towards the heat exchanger and determine their size, we have recorded spray by the high-speed digital video camera with frame frequency F = 5 kHz [1]. The size and velocity of droplets in the flow were determined by the results of optic measurements with the help of special software “Phantom Control”. The picture of two-pulse droplet train in the drift space between the heat exchanger and nozzle of a single valve is shown in Fig. 4. Without the co-current air flow deceleration rates for the droplets of different sizes differ, and the large droplets are grouped in the “head” of the pulse, whereas the small ones are grouped in its “tail”, and this causes nonuniform flow density in space to the heat exchanger surface. Accordingly, the heat exchanging surface will be washed periodically by the large droplets at first, and then by the small liquid droplets. According to analysis of video recording, when the liquid jets are ejected from four sprayer holes they are separated into droplets with the length of 200 ÷ 500 um at the initial region of motion (L = 60 mm). Droplet splitting continues during the motion towards the heat exchanger. Near the plate surface (L = 210 mm) two main droplets sizes are observed: large droplets of 120 ÷ 150 um and small ones of 45 ÷ 50 um. Data analysis demonstrates that without the co-current air flow the droplet train extends by the factor of 3-4 during its motion.

Optic measurements were supplemented by data obtained at bombardment of the local pulsation sensor by the flow droplets. A pulse signal from the pulsation sensor allowed us to measure distribution of droplet concentration in the train and the train velocity via the time of drift from the source to the sensor. For these measurements we have used the piezoelectric pulsation sensor with the diameter of ∅10 mm, sensitivity of S = 10 mV·Pa^{-1}, and width of frequency band F_i = (50-15000) Hz. The measurement error for pulsation amplitude was ~5 %. The oscillogram of sensor signal at inlet liquid pressure P_l = 0.2 MPa and air pressure at the nozzle inlet P_g = 0.2 MPa is shown in Fig. 6. Analysis of data from the pulsation sensor proves the results of high-speed recording. The control pulse for the opening of electromagnetic valve is combined with the sensor signal in Fig. 5. It is obvious that in comparison with the control pulse duration of the sensor signal is three times

longer, and this proves extension of the droplet train on the way from the source to the heat exchanger surface. The steep front of the sensor signal means that the large droplets with a significant store of kinetic energy are in the "head" of droplet area. The descending part of the signal is gentle, and this testifies that small droplets with a low level of kinetic energy move behind the "head" of the droplet area. According to optic observations, droplet separation depends on many factors, and the main among them are the pulse parameters of spray, distance from the source, and velocity of the co-current air flow.

A relative change in the value of spray droplet pulse at continuous and pulse operation is shown in Fig. 6 with and without the co-current air flow. The experimental integral pulse of the two-phase flow falling on the sensor is $K = (\pi R_o^2)^{-1} \left| \sum_{i=1}^{n} m_{Pi} V_{Pi} \right|$ where R_o is radius of piezosensor, m_{Pi} and Vp_i are mass and longitudinal component of the droplet velocity [3]. Experimental data analysis testifies a change in relative pulse $K \cdot K_o^{-1}$ along the flow trajectory (K_o is pulse of spray falling on the sensor at the source outlet). In space between the source and heat exchanger there is the total tendency to reduction of this parameter with continuous and pulse spray motions. The co-current air flow in the continuous spray reduces ratio $K \cdot K_o^{-1}$ significantly. Simultaneously, there is a bright maximum at some distance from the nozzle observed in the pulse spray, and this proves the effect of droplet transformation into "braid" and maximal droplet grouping in this zone. It is important that for different initial velocity of the flow and frequency parameters of spray the area with high concentration of aerosol changes both by the coordinate and amplitude.

The frequency spectrum of energy pulsations of the pulse spray shown in Fig. 7 allows us to determine the contribution of various mechanisms effecting its inner structure at propagation. According to analysis of spectrum of energy pulsations in range $F = 2 \div 3200$ Hz, the main contribution is in frequency range $F = 0.5 \div 1$ kHz. The spectrum of energy pulsations of the droplet train in the low-frequency area ($F_{Lo} = 10 \div 150$ Hz) relates to frequency of pulse repetition and their duration; the high-frequency range of spectrum is formed by the action of separate droplets and their short groups ($F_{Hi} = 0{,}5 \div 1$ kHz). In Fig. 7 this range is shown for two sensor positions (0.03 and 0.21 m) relative to the source. As it follows from the figure, at motion of the spray pulse along the axis in low-frequency (F_{Lo}, ranges A and B) and high-frequency (F_{Hi}, ranges C and D) zones the maximums shift towards the range of pulsation spectrum with higher frequencies, and this indicates the effect of droplet grouping.

It is obvious that this droplet redistribution in alternating spray pulses changes the character of liquid film formation considerably and influences surface heat and mass transfer in different manners.

According to the above material, thorough analysis of mechanics of multiphase flow complex structures and their interaction with different objects for intensive heat transfer is possible only with application of modern automated investigation setups and computation systems, which allow data registration and optimization of research under the real time conditions.

The work financially supported by the Russian Foundation for Basic research (project No. 09-08-00197-a).

Nomenclature

B	magnetic induction [T]
D	electric induction [C]
E	electric field strength [$V \cdot m^{-1}$]
F	frequency [Hz]
H	magnetic field strength [$A \cdot m^{-1}$]
K	spray pulse [$kg \cdot m \cdot s^{-1}$]
L	distance from spray source to heat exchanger [m]
R_0	radius of piezosensor [m]
T	duration of valve opening [s]
P	pressure [Pa]
S	sensitivity of piezoelectric sensor [$mV \cdot Pa^{-1}$]
V	velocity [$m \cdot s^{-1}$]
ε_0	electric constant (8.85×10^{-12}) [$F \cdot m^{-1}$]
ε	medium permeability
ω	energy density in electromagnetic wave
μ_0	magnetic permeability of medium (1.2×10^{-12}) [$H \cdot m^{-1}$]
μ	magnetic permeability of medium

Subscripts

g	gas
I	pulse
l	liquid

p droplet
Lo lower part of spectrum
Hi upper part of spectrum

References

[1] Nazarov A.D., Serov A.F. and Bodrov M.V., *Technical Physics,* Vol. 55, № 5: 724-727 (2010).
[2] Nazarov A.D., *Instruments and Experimental Techniques,* Vol. 53, № 3: 454-456 (2010).
[3] Landau L.D. and Lifshits E.M. *Mechanics. Electrodynamics*, Moscow: Nauka, 1969, p. 272.
[4] Kaye G.W. and Lables T.H., *Tables of Physical and Chemical Constants*, Moscow: Gos. Izd. Fiz.-mat. Lit., 1962, p. 248.

Figure 1. Construction of pulse spray source and its elements. a - appearance; b – outlet panel of air and liquid-droplet phases; c – liquid electromagnetic valve

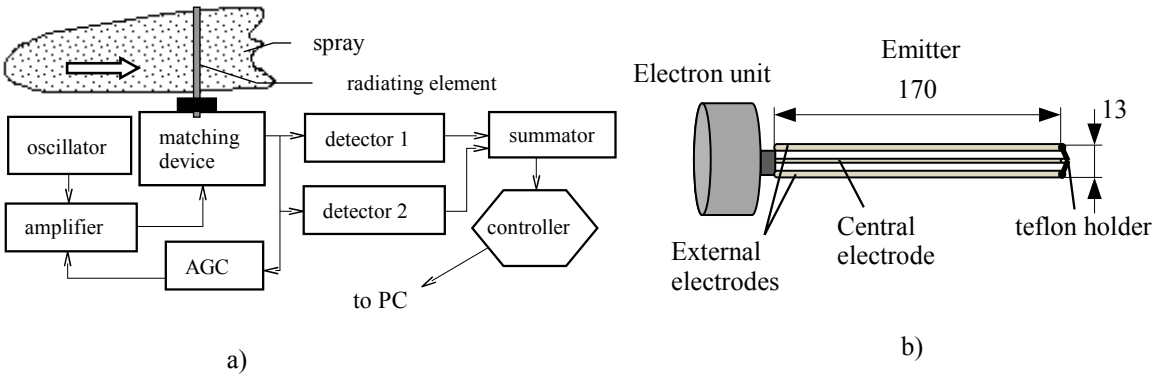

Figure 2. a – structural scheme of meter; b – construction of emitter

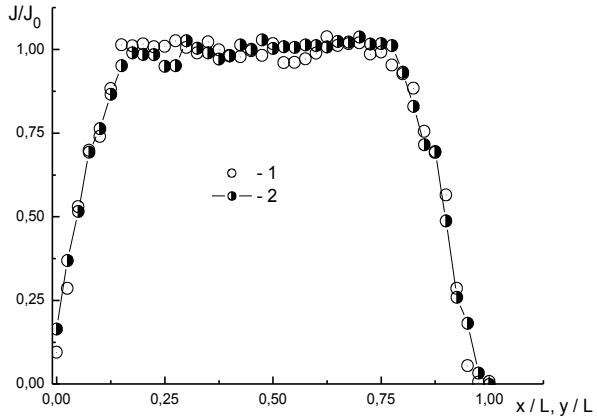

Figure 4. Distribution of droplet phase concentration in to orthogonal directions: 1 − vertical; 2 – horizontal

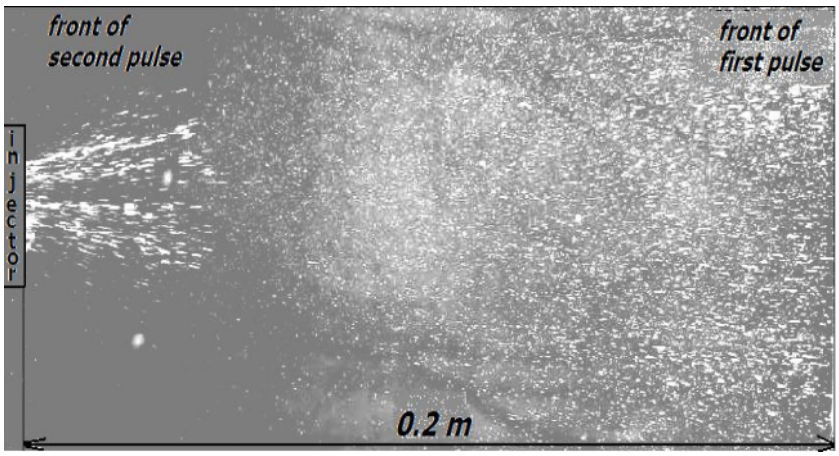

Figure 5. Visualization of pulse spray development. Period between pulses – 0.01 s

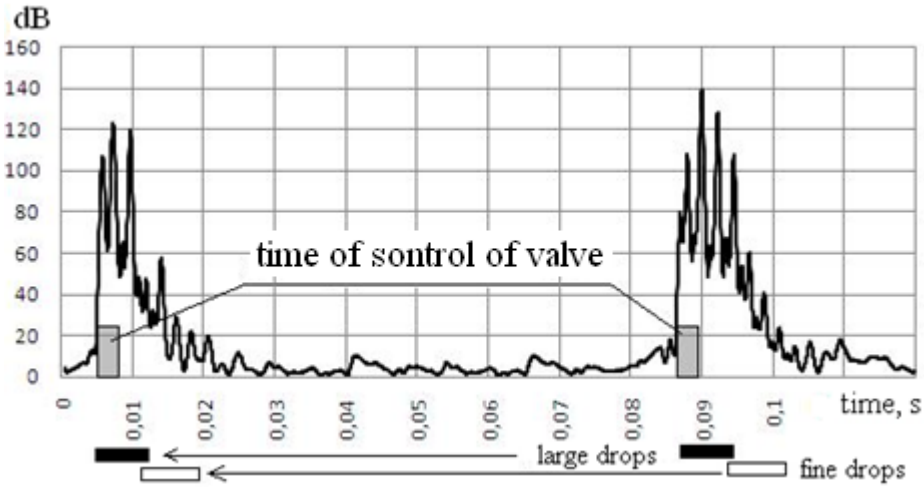

Figure 6. Oscillogram of flow pressure pulsations (Duration of valve pulse T_i =3 ms, frequency F_i =10 Hz, large droplets, D ~ (120-150) μm; small droplets d ~ (45-50) μm.)

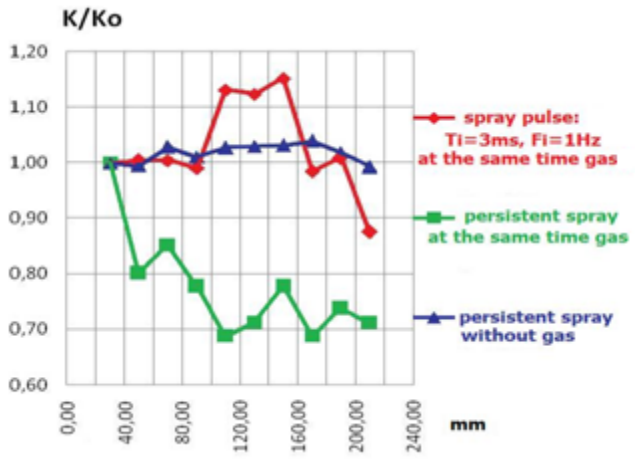

Figure 7. Distribution of relative pulse of the droplet flow along the spray axis. (K_0 – pulse spray at the nozzle outlet)

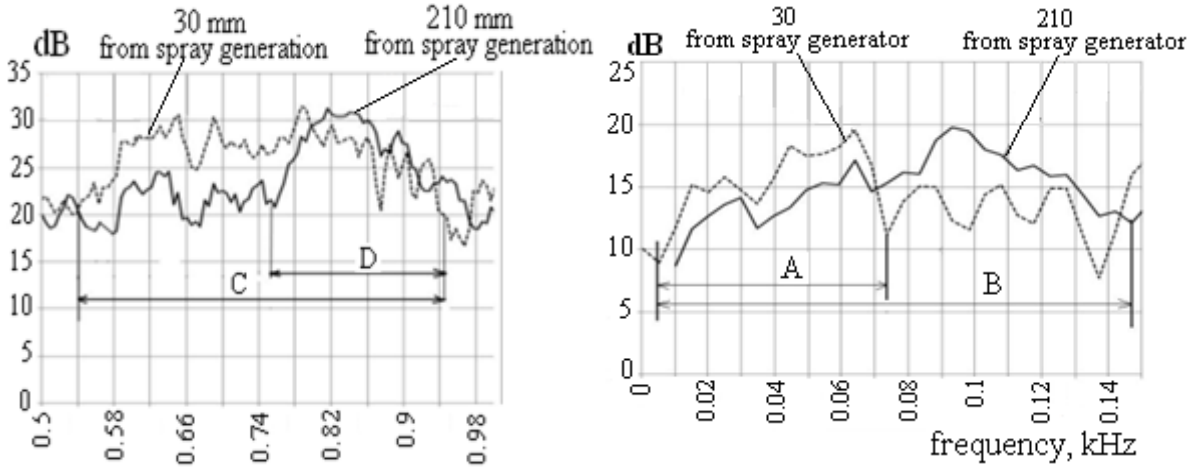

Figure 8. Frequency spectrum of energy pulsations of pulse spray for two positions of the probe. Experimental parameters: T_i = 0.003s, F_i = 10 Hz, P_l = 2 atm, P_g = 1 atm.
a - low-frequency range; b - high-frequency range